

Small-Molecule Turn-On Fluorescent Probes for RDX

Lorenzo Mosca, Sara Karimi Behzad, and Pavel Anzenbacher, Jr.*

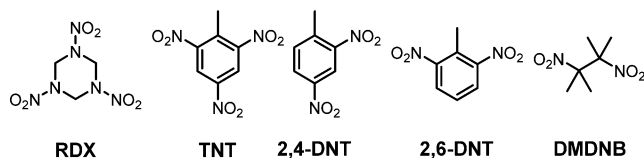
Department of Chemistry and Center for Photochemical Sciences, Bowling Green State University, Bowling Green, Ohio 43403, United States

S Supporting Information

ABSTRACT: New fluorescent probes have been tested for their ability to detect nitramine (RDX) and nitroaromatic (TNT) explosives. The probes display turn-on behavior upon exposure to RDX, while their fluorescence is dramatically reduced by the presence of TNT and other nitroaromatic compounds. The probes are applicable in qualitative assays that can distinguish between RDX and TNT as well as acidity and formaldehyde vapors.

National and global security concerns over the use of explosives in terrorism are increasing, and so is the demand for faster, less expensive, and possibly stand-off detection of energetic materials.¹ The use of 1,3,5-trinitroperhydro-1,3,5-triazine (RDX) in explosives is second only to that of 2,4,6-trinitrotoluene (TNT) (Chart 1). RDX is the most used explosive in plastic formulations, i.e., composition-C (C4), Semtex, etc., in civilian and military applications.

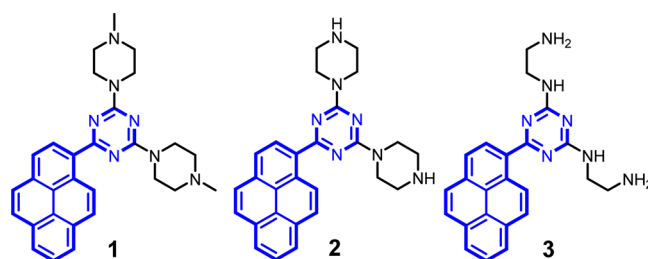
Chart 1. Analytes Used in This Study



The current standard in the detection of explosives is based on ion-mobility spectrometers (IMs).^{1–3} Methods for the detection of RDX by means of immunoassay protocols,^{4,5} Raman spectroscopy,⁶ and surface plasmon resonance⁷ have been reported. Such methods, however, need expensive instrumentation, are sensitive to contaminants, or may not be amenable to stand-off detection. Optical detection, such as colorimetric or fluorimetric methods, offers advantages such as rapid response times, simple and reliable instrumentation, and the possibility for stand-off detection. Colorimetric methods⁸ have been explored but appear to suffer from poor selectivity and sensitivity. Anslin⁹ reported a supramolecular cross-reactive colorimetric array that can discriminate between nitroaromatic, nitramine, and nitrate ester explosives. Numerous fluorescence-based approaches¹⁰ based on quenching of emission have been demonstrated, such as Troglor's silafluorene-based polymers,¹¹ Tanaka's phosphole oxide,¹² Dichtel's microporous tris(phenylene)vinylene polymer,¹³ and Anslin's cross-reactive arrays.^{14,15} As a general concept, sensors based on turn-on behavior are preferable to ones displaying fluorescence quenching. Photolytic cleavage of the N–NO₂

bond to yield NO₂[−] and NO₂ from RDX has been successfully exploited by Swager to generate fluorescent molecules via photo-oxidation or photonitration of acridine derivatives.^{16,17} Herein we report a recent advance in the turn-on detection of RDX with three new fluorescent probes (Chart 2).

Chart 2. Structures of Probes 1–3



Inspired by earlier works on the decomposition of RDX,^{18–20} we sought probes that can detect one or more of its decomposition products. Here, a pyrene fluorophore has been appended with a triazine ring bearing two amino-derivative substituents. The quantum yields reflect the donating ability of the amino groups in the photoinduced electron transfer (PET) quenching of the pyrene emitter (1 = 1.0%; 2 = 0.4%; 3 = 10.8%). These amine substituents were chosen to impart increasing basicity/nucleophilicity to the probe. This aspect is of crucial importance since RDX is stable under acidic conditions but undergoes rapid hydrolytic cleavage under basic conditions.²⁰

Upon titration of probe 3 with RDX in MeCN solution, the emission intensity of the fluorophore is enhanced up to 3-fold (Figure 1). An apparent association constant $K = 1968 \pm 139 \text{ M}^{-1}$ was determined by assuming a 1:1 binding model.

Hawari²⁰ showed that the base-promoted hydrolysis of RDX provides intermediate I, which further decomposes to give 4-nitro-2,4-diazabutanal (II), HCHO, and N₂O as major products with molar yields close to theoretical (Scheme 1). We assume that compound II, N₂O, and NO₂[−] do not interact with the probes. Instead, HCHO can react with primary and secondary amino groups in the probes to form imine/iminium compounds.

Upon formation of the imine, the energy of the nitrogen atom lone pair is lowered, and the PET quenching becomes less efficient. Thus, the presence of RDX also enhances the emission of probes 1 and 2. However, upon titration with a

Received: May 4, 2015

Published: June 13, 2015

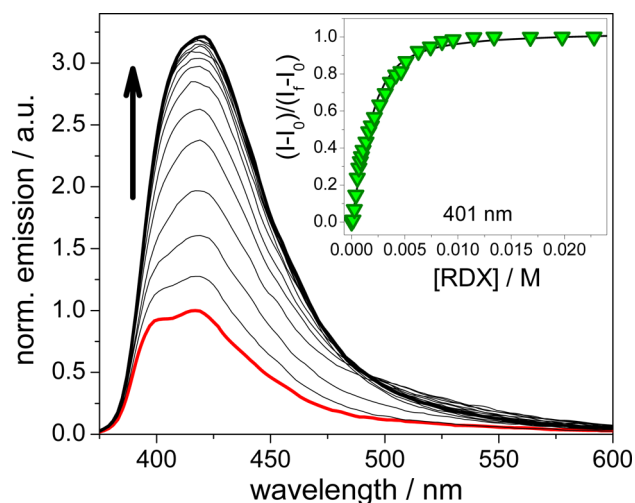
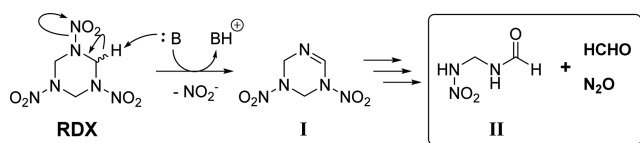


Figure 1. Titration of probe 3 (2.861×10^{-6} M) with RDX in MeCN ($\lambda_{\text{exc}} = 355$ nm). The inset shows the titration isotherm (\blacktriangledown) and fitting curve (—) calculated assuming a 1:1 binding model.

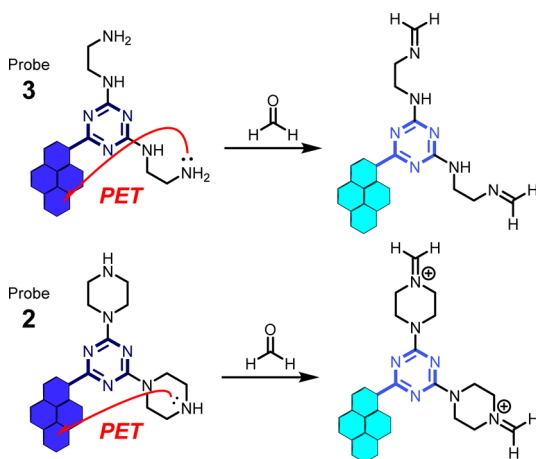
Scheme 1. Base-Promoted Cleavage of RDX and Major Products of the Hydrolysis



strong acid (trifluoroacetic acid) and vapors of formaldehyde, probes 1–3 respond to protonation with a turn-on response, while only probes 2 and 3 respond to formaldehyde (see section 2 in the Supporting Information). We believe that the formation of the imine on the terminal $-\text{NH}_2$ groups in probe 3 and the formation of the iminium cation on the secondary amines in probe 2 render the PET from the nitrogen atoms to the pyrene unfavorable (Scheme 2). However, formaldehyde shows no effects on the fluorescence of probe 1, so the turn-on behavior can be explained by protonation of the tertiary amines upon deprotonation from RDX.

The products of the reactions of probes 3 and 2 with RDX were identified in the MALDI-TOF spectrum obtained by analyzing a sample containing both probes and RDX (see

Scheme 2. Proposed Turn-On Mechanism for 3 and 2



section 3 in the Supporting Information). The peaks at m/z 398.4, 410.4, and 422.4 correspond to protonated 3 ($[\text{M} + \text{H}]^+$), the monoimino derivative of 3 H^+ , and the protonated bisimino derivative of 3, respectively. In the case of probe 2, two main peaks were observed at m/z 450.1 and 462.0, corresponding to protonated 2 ($[\text{M} + \text{H}]^+$) and the monoiminium derivative of 2, respectively. The presence of these mass signatures confirms our hypothesis that imino derivatives of probes 2 and 3 are formed upon reaction with RDX.

TNT is the most used energetic material in legally produced explosives and in improvised explosive devices (IEDs). Our group recently demonstrated the use of small-molecule fluorescent and luminescent sensors for nitroaromatic explosives detection.^{21–23} Titration of probes 1–3 with 2,4-dinitrotoluene (2,4-DNT), 2,6-dinitrotoluene (2,6-DNT), and TNT in CH_2Cl_2 showed quenching behavior.

The reaction between nitroaromatic compounds and nucleophilic reagents has been reported previously²⁴ and involves aromatic nucleophilic attack at one of the electron-deficient positions on the aromatic ring to form a stable Meisenheimer complex. It has been suggested that a Förster resonance energy transfer (FRET) mechanism is responsible for the quenching of luminescence in the presence of the TNT–amine Meisenheimer complex (section 6 in the Supporting Information).^{25,26} The analysis of titration isotherms and linearized plots showed that neither a 1:1 binding model or a purely dynamic quenching regime are sufficient in describing the titrations with nitro compounds. We assumed that binding occurs simultaneously with purely dynamic (collisional) quenching. The quenching constants (Table 1)

Table 1. Values of Quenching Constants (in M^{-1}) for Probes 1–3^a

	1	2	3
TNT	536	1092	3513
2,6-DNT	866	752	2399
2,4-DNT	534	513	3322
DMDNB	19.0 ^b	$>10^4$	$>10^4$

^aAll errors were below 15%. ^bThe quenching constant was calculated using a dynamic-quenching model only.

were determined by fitting the titration data using a modified Stern–Volmer equation that also takes into account static (bound) effects.²³ The magnitude of the quenching constants follows the order $\text{TNT} > 2,6\text{-DNT} > 2,4\text{-DNT}$ and the nucleophilic character of the probes ($3 > 2 > 1$). Surprisingly, 2,3-dimethyl-2,3-dinitrobutane (DMDNB) showed extremely high affinities for probes 2 and 3. We suggest the formation of a loosely bound complex held together by hydrogen-bonding interactions between the $-\text{NH}$ groups of the probes and the $-\text{NO}_2$ groups of DMDNB.

In order to evaluate the ability of probes 1–3 to discriminate between different analytes, including RDX and TNT, we performed a qualitative assay comprising the two explosives, DMDNB, and formaldehyde and trifluoroacetic acid as simulants of contamination. The RGB values obtained from three separate acquisition channels were utilized to build a color image, as shown in Figure 2. The tridimensional surface plot shows that TNT effectively quenches the fluorescence of the probes while RDX enhances the fluorescence of probes 2 and 3. Moreover, the emission of probe 2 and RDX shows a

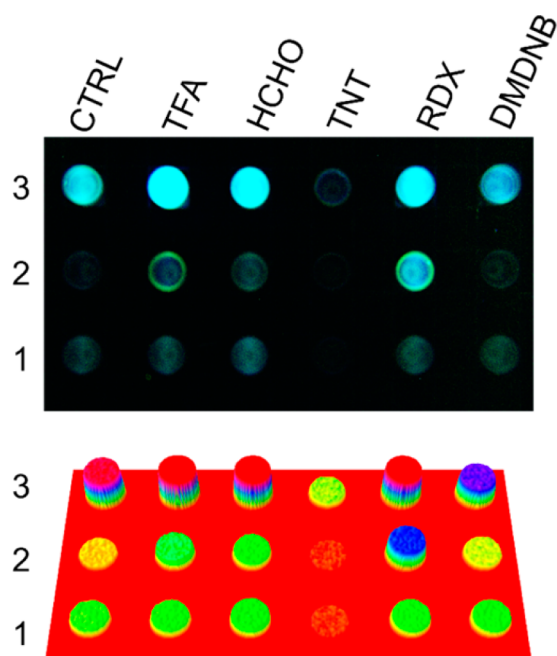


Figure 2. (top) RGB-processed image of the qualitative assay involving probes 1–3 and several analytes. (bottom) Tridimensional surface plot of the same image.

marked increase in intensity in the green channel, which constitutes a key identification signature.

Also, it is possible to see how formaldehyde does not considerably enhance the emission of probes 1 and 2, while an acidic environment barely affects the emission of probe 2. These changes in the emissions of the probes constitute a fingerprint signature characteristic of each contaminant considered and represent a promising approach in the qualitative detection of explosives.

This work demonstrates the use of new small-molecule probes for sensing of the explosive RDX via a turn-on mechanism. These small-molecule fluorescent probes were found to be sensitive to the presence of TNT and other nitroaromatics as well, with a turn-off response. Furthermore, a qualitative assay allows for visual detection of the presence of five different analytes, while analyte-specific variations in the responses of the three probes allow the discrimination of RDX from acidic impurities and formaldehyde. The probes for RDX presented here are far superior to others examples reported in the literature because they rely on a turn-on of fluorescence^{12,14} and because the enhancement of fluorescence is caused by the formaldehyde generated by the decomposition of nitramines instead of NO_x species, which are ubiquitous pollutants.^{17,18} As reported in our previous works, the deployment of sensors for explosives is facilitated by the use of suitable matrices. These probes could be doped into polymer nanofibers²¹ to improve the mass transfer between the contaminated sample and the sensing elements and reduce the response time, while polymeric matrices with different functionalities and/or polarities might improve the selectivity toward one or more analytes.²³

■ ASSOCIATED CONTENT

📄 Supporting Information

Synthetic details, fluorescence titrations, MS data, and additional reaction schemes. The Supporting Information is

available free of charge on the ACS Publications website at DOI: 10.1021/jacs.5b04643.

■ AUTHOR INFORMATION

Corresponding Author

*pavel@bgsu.edu

Notes

The authors declare no competing financial interest.

■ ACKNOWLEDGMENTS

P.A. gratefully acknowledges financial support from the Office of Naval Research (Contract W909MY-12-C-0031) and NSF (DMR-1006761).

■ REFERENCES

- (1) *Aspects of Explosives Detection*, 1st ed.; Marshall, M., Oxley, J. C., Eds.; Elsevier: Amsterdam, 2009.
- (2) Moore, D. S. *Rev. Sci. Instrum.* **2004**, *75*, 2499–2512.
- (3) Tabrizchi, M.; Ilbeigi, V. *J. Hazard. Mater.* **2010**, *176*, 692–696.
- (4) Charles, P. T.; Kusterbeck, A. W. *Biosens. Bioelectron.* **1999**, *14*, 387–396.
- (5) Desmet, C.; Blum, L. J.; Marquette, C. A. *Anal. Chem.* **2012**, *84*, 10267–10276.
- (6) Moros, J.; Laserna, J. J. *Anal. Chem.* **2011**, *83*, 6275–6285.
- (7) Riskin, M.; Tel-Vered, R.; Willner, I. *Adv. Mater.* **2010**, *22*, 1387–1391.
- (8) Germain, M. E.; Knapp, M. J. *Chem. Soc. Rev.* **2009**, *38*, 2543–2555.
- (9) Ponnuru, A.; Edwards, N. Y.; Anslyn, E. V. *New J. Chem.* **2008**, *32*, 848–855.
- (10) Meaney, M. S.; McGuffin, V. L. *Anal. Bioanal. Chem.* **2008**, *391*, 2557–2576.
- (11) Sanchez, J. C.; Troglor, W. C. *J. Mater. Chem.* **2008**, *18*, 3143–3156.
- (12) Shiraishi, K.; Sanji, T.; Tanaka, M. *ACS Appl. Mater. Interfaces* **2009**, *1*, 1379–1382.
- (13) Gopalakrishnan, D.; Dichtel, W. R. *J. Am. Chem. Soc.* **2013**, *135*, 8357–8362.
- (14) Hughes, A. D.; Glenn, I. C.; Patrick, A. D.; Ellington, A.; Anslyn, E. V. *Chem.—Eur. J.* **2008**, *14*, 1822–1827.
- (15) Ponnuru, A.; Anslyn, E. V. *Supramol. Chem.* **2010**, *22*, 65–71.
- (16) Andrew, T. L.; Swager, T. M. *J. Am. Chem. Soc.* **2007**, *129*, 7254–7255.
- (17) Andrew, T. L.; Swager, T. M. *J. Org. Chem.* **2011**, *76*, 2976–2993.
- (18) Epstein, S.; Winkler, C. A. *Can. J. Chem.* **1951**, *29*, 731–733.
- (19) Hoffsommer, J. C.; Kubose, D. A.; Glover, D. J. *J. Phys. Chem.* **1977**, *81*, 380–385.
- (20) Balakrishnan, V. K.; Halasz, A.; Hawari, J. *Environ. Sci. Technol.* **2003**, *37*, 1838–1843.
- (21) Anzenbacher, P., Jr.; Mosca, L.; Palacios, M. A.; Zyryanov, G. V.; Koutnik, P. *Chem.—Eur. J.* **2012**, *18*, 12712–12718.
- (22) Mosca, L.; Koutnik, P.; Lynch, V. M.; Zyryanov, G. V.; Esipenko, N. A.; Anzenbacher, P., Jr. *Cryst. Growth Des.* **2012**, *12*, 6104–6109.
- (23) Mosca, L.; Khnayzer, R. S.; Lazorski, M. S.; Danilov, E. O.; Castellano, F. N.; Anzenbacher, P., Jr. *Chem.—Eur. J.* **2015**, *21*, 4056–4064.
- (24) Oxley, J. C.; Smith, J. L.; Yue, J.; Moran, J. *Propellants, Explos., Pyrotech.* **2009**, *34*, 421–426.
- (25) Gao, D.; Wang, Z.; Liu, B.; Ni, L.; Wu, M.; Zhang, Z. *Anal. Chem.* **2008**, *80*, 8545–8553.
- (26) Geng, J.; Liu, P.; Liu, B.; Guan, G.; Zhang, Z.; Han, M.-Y. *Chem.—Eur. J.* **2010**, *16*, 3720–3727.